

# Mechanism and Specificity of Lanthanide Series Cation Transport by Ionophores A23187, 4-BrA23187, and Ionomycin

Exing Wang,\* Richard W. Taylor,# and Douglas R. Pfeiffer\*

\*Department of Medical Biochemistry, The Ohio State University, Columbus, Ohio 43210, and #Department of Chemistry and Biochemistry, University of Oklahoma, Norman, Oklahoma 73019 USA

**ABSTRACT** A23187, 4-BrA23187, and ionomycin transport several lanthanide series trivalent cations at efficiencies similar to  $\text{Ca}^{2+}$ , when compared at cation concentrations of  $\sim 10^{-5}$  M, ionophore concentrations of  $\sim 10^{-6}$  M, and a pH of 7.00. Selectivity sequences and the range of relative rates are as follows: A23187,  $\text{Nd}^{3+} > \text{La}^{3+} > \text{Eu}^{3+} > \text{Gd}^{3+} > \text{Er}^{3+} > \text{Yb}^{3+} > \text{Lu}^{3+}$  ( $\sim 34$ -fold); 4-BrA23187,  $\text{Nd}^{3+} > \text{Eu}^{3+} > \text{Gd}^{3+} > \text{La}^{3+} > \text{Er}^{3+} > \text{Yb}^{3+} > \text{Lu}^{3+}$  ( $\sim 34$ -fold); ionomycin,  $\text{La}^{3+} > \text{Yb}^{3+} > \text{Nd}^{3+} > \text{Lu}^{3+} > \text{Er}^{3+} > \text{Eu}^{3+} > \text{Gd}^{3+}$  ( $\sim 4$ -fold). At concentrations between 9 and 250  $\mu\text{M}$ ,  $\text{La}^{3+}$  is transported by an electroneutral mechanism, predominately through mixed complexes of the type (ionophore)<sub>2</sub>La·OH (A23187 and 4-BrA23187) or (ionophore)La·OH (ionomycin), when no membrane potential is present. For all three ionophores, an induced potential of  $\sim 160$  mV accelerates transport by  $\sim 50$ –100%. However, measured values of  $\text{H}^+/\text{La}^{3+}$  exchange indicate that only 4-BrA23187 displays a significant electrogenic activity under these conditions. At a  $\text{La}^{3+}$  concentration of 17 mM, transport by all three ionophores is electroneutral and apparently occurs through complexes of type (ionophore)<sub>3</sub>La (A23187 and 4-BrA23187) or (ionophore)La·OH (ionomycin). Analysis of these patterns in a context of comproportionation equilibria involving the transporting species and free  $\text{La}^{3+}$  indicates that the species containing three ionophore molecules are formed on the membrane when aqueous phase solution conditions would strongly favor a 1:1 complex, based upon previous studies in solution. The implications of this and other findings are discussed.

## INTRODUCTION

We have recently utilized a phospholipid vesicle system to investigate the mechanism (Erdahl et al., 1994, 1995; Thomas et al., 1997) and specificity (Erdahl et al., 1996) of cation transport catalyzed by the carboxylic acid ionophores A23187, 4-BrA23187, and ionomycin (see Fig. 1 for structures). These studies verified and extended a model for  $\text{Ca}^{2+}$  transport proposed earlier (Pfeiffer et al., 1978; Shastri et al., 1987; Fasolato et al., 1989), in which the cation is exchanged for  $2\text{H}^+$  through a process that is strictly electroneutral. The transporting species are 2:1 complexes (ionophore: $\text{Ca}^{2+}$ ) (A23187 and 4-BrA23187) or a 1:1 complex (ionomycin). The model has not been tested for the transport of other cations, although aspects of the existing data suggest that some are transported by alternative mechanisms, and that these are important for establishing selectivity. In particular, 4-BrA23187 is highly selective for the transport of  $\text{Zn}^{2+}$  and  $\text{Mn}^{2+}$ , compared to  $\text{Ca}^{2+}$ , with selectivity values in excess of  $10^3$  obtained under optimal conditions (Erdahl et al., 1996). Neither A23187 nor ionomycin displays analogous properties (Erdahl et al., 1996). Compared to A23187, the high selectivity of 4-BrA23187 reflects decreased activity as a  $\text{Ca}^{2+}$  ionophore, whereas the activities for  $\text{Zn}^{2+}$  and  $\text{Mn}^{2+}$  are similar for both compounds (Erdahl et al., 1996). To explain the low  $\text{Ca}^{2+}$  transport activity of 4-BrA23187, we proposed that interli-

gand hydrogen bonds (Pfeiffer et al., 1976; Smith et al., 1976), which stabilize the (A23187)<sub>2</sub>Ca complex relative to the (A23187)Ca<sup>+</sup> complex, are weakened by the introduction of bromine at position 4. Because the charge-bearing 1:1 complex is not a transporting species for either ionophore (Erdahl et al., 1994, 1995), destabilizing the 2:1 complex reduces activity as a  $\text{Ca}^{2+}$  ionophore. To explain the similar activities of A23187 and 4-BrA23187 as ionophores for  $\text{Zn}^{2+}$  and  $\text{Mn}^{2+}$ , we proposed that these cations are transported in part by both compounds as uncharged mixed complexes of the type (ionophore)M·OH. In that case, weakening the interligand hydrogen bonds that stabilize 2:1 complexes would have less effect on the rate of transport. Thus an alternative transport mechanism for  $\text{Zn}^{2+}$  and  $\text{Mn}^{2+}$  may underlie a selective transport of these cations by 4-BrA23187 (Erdahl et al., 1996).

Lanthanide series trivalent cations ( $\text{Ln}^{3+}$ ) are bound (Puskin et al., 1975; Pfeiffer and Lardy, 1976; Albin et al., 1984; Chapman et al., 1990b) and transported (Hunt, 1975; Hunt et al., 1978, 1982; Amellel et al., 1983; Grandjean et al., 1984; Shastri et al., 1987) by A23187, suggesting that additional transporting species and mechanisms may exist, at least for that ionophore. However, in the existing studies, NMR was used to monitor transport, which was seen as a change in phospholipid headgroup signals reflecting changing concentrations of paramagnetic  $\text{Ln}^{3+}$  on opposing sides of the membrane. While elegant in many regards, this method is not well suited to detailed investigations employing a range of conditions, because of low sensitivity and for other reasons. Accordingly, the available data are not sufficient to formulate specific mechanisms for  $\text{Ln}^{3+}$  transport, and are conflicting in some aspects. As an example, the stoichiometry (ligand:metal) of the transporting species is in

Received for publication 14 August 1997 and in final form 12 May 1998.

Address reprint requests to Dr. Douglas R. Pfeiffer, Department of Medical Biochemistry, The Ohio State University, 310A Hamilton Hall, 1645 Neil Avenue, Columbus, OH 43210-1218. Tel.: 614-292-5451; Fax: 614-292-4118; E-mail: pfeiffer.17@postbox.acs.ohio-state.edu.

© 1998 by the Biophysical Society

0006-3495/98/09/1244/11 \$2.00

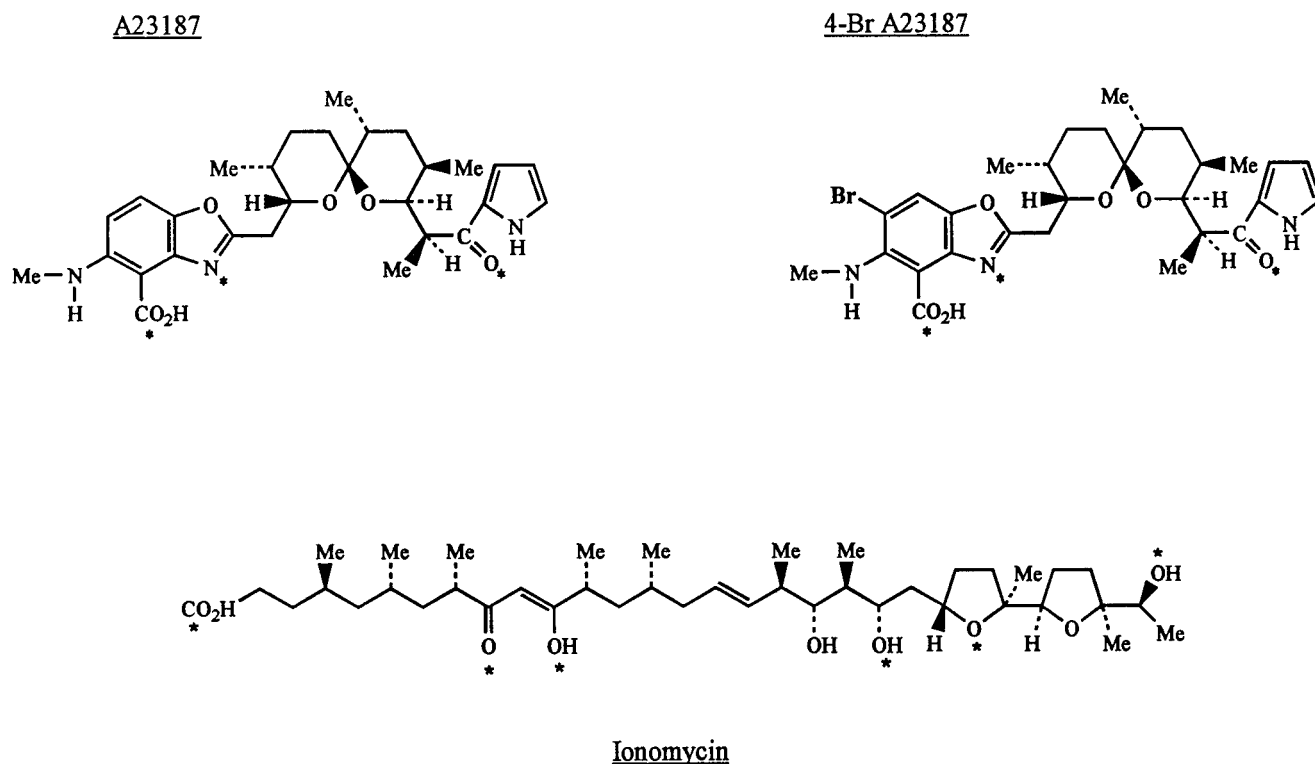


FIGURE 1 Structures of A23187, 4-BrA23187, and ionomycin. Compounds are shown in their free acid forms, as opposed to the ionized forms present in the cation complexes. Ligand donor atoms are marked with an asterisk.

doubt; it is placed at 1:1 by Hunt and co-workers (Hunt, 1975; Hunt et al., 1978) and at 2:1 by Shastri et al. (1987). In addition, it is not clear how or if electroneutrality is maintained, and there are no data that reveal transport selectivity for  $\text{Ln}^{3+}$ , compared to cations that carry a different charge.

In the present report we describe the use of phospholipid vesicles loaded with the chelating indicator Quin-2 to further characterize the transport properties of divalent cation ionophores for  $\text{Ln}^{3+}$ . This approach overcomes several limitations of the NMR methods used previously, yielding results that provide a more complete view of factors that govern the transport mode and selectivity of these compounds. In particular, it is shown that transport of  $\text{Ln}^{3+}$  is predominately an electroneutral process that occurs via mixed complexes that contain  $\text{OH}^-$ , supporting the proposed basis for the high transport selectivity of 4-BrA23187 for  $\text{Zn}^{2+}$  and  $\text{Mn}^{2+}$ . The results also show that  $\text{Ca}^{2+}$  ionophores are substantially selective for the transport of particular  $\text{Ln}^{3+}$  within a set, and that the rates are similar to the rate of  $\text{Ca}^{2+}$  transport under some conditions. Aspects of these findings have been presented in abstract form (Wang et al., 1996).

## MATERIALS AND METHODS

### Reagents

Synthetic 1-palmitoyl-2-oleoyl-*sn*-glycerophosphatidylcholine (POPC) was obtained from Avanti Polar Lipids. Purity was confirmed by thin-layer

chromatography before use. A23187, 4-BrA23187, and ionomycin were obtained from Sigma or Calbiochem and were used without further purification. Stock solutions in ethanol were standardized spectrophotometrically using the following extinction coefficients: 4-BrA23187 ( $\Sigma_{290} = 15,600$ ); A23187 ( $\Sigma_{278} = 21,040$ ); ionomycin ( $\Sigma_{278} = 13,560$ ). Quin-2 ( $\text{K}^+$ ) from Sigma was purified by passage over Chelex 100 resin (100–200 mesh) in the  $\text{Cs}^+$  form as described previously (Erdahl et al., 1994). Stock solutions of  $\text{CaCl}_2$  (ultrapure grade from Alfa Products) were standardized by titration with a primary standard EDTA solution (Vogel, 1961). Lanthanide series metal oxides, also ultrapure, were obtained from Alfa products or Aldrich Chemical Co. Samples were reacted with an excess of 1 M perchloric acid, filtered, and then standardized by titration with EDTA. Excess hexamethylenetetramine, pH 5.5–6.0, was employed to buffer the unknown samples, and the titration endpoints were indicated by xylene orange (Lyle et al., 1963).

### Preparation of phospholipid vesicles

POPC vesicles loaded with Quin-2 were prepared by freeze-thaw extrusion as previously described (Erdahl et al., 1994, 1995). The resulting preparations were applied to Sephadex G-50 mini-columns and eluted by low-speed centrifugation (Fry et al., 1978), to replace the external medium with 10 mM HEPES ( $\text{Cs}^+$ ) buffer, pH 7.00 (Erdahl et al., 1994, 1995). The nominal concentration of POPC in the final preparations was determined as lipid phosphorus (Bartlett, 1959) and was near 80 mM. The average diameter of these vesicles is 71 nm, as determined by freeze-fracture electron microscopy (Chapman et al., 1990a). They contain entrapped solutes at the following concentrations; Quin-2,  $10.5 \pm 0.8$  mM; HEPES,  $33.7 \pm 7.6$  mM (pH  $\approx 7.4$ ); and  $\text{Cs}^+$ ,  $60 \pm 5$  mM (Erdahl et al., 1995). Specific values for Quin-2 and  $\text{Cs}^+$  were determined for each preparation, by spectral titration and atomic absorption, respectively (Erdahl et al., 1994, 1995).

Vesicles loaded with  $\text{La}^{3+}$  were prepared and purified in an analogous way, except that 5 mM  $\text{LaCl}_3$  was present in the formation medium, rather

than Quin-2. In addition, the HEPES buffer used in the Quin-2 containing preparations was replaced with 2-(*N*-morpholino)ethanesulfonic acid at pH 6.00. To determine entrapped  $\text{La}^{3+}$ , an aliquot of the final preparation was lysed with deoxycholate (Erdahl et al., 1994) and then titrated with a standard solution of Quin-2, while monitoring formation of the Quin-2:  $\text{La}^{3+}$  complex by difference spectroscopy (see below).  $\text{La}^{3+}$  is tightly bound by Quin-2, forming a 1:1 complex with a stability constant of  $\sim 10^{12} \text{ M}^{-1}$  (Jones et al., 1992; Yuchi et al., 1993). Accordingly, a sharp end point is obtained, which is seen as an inflection point in plots of Quin-2 difference absorbance versus  $\text{La}^{3+}$  concentration. This method gave an internal  $\text{La}^{3+}$  concentration of  $16.9 \pm 0.5 \text{ mM}$ , similar to the level of  $\text{Ca}^{2+}$  entrapped by an analogous procedure (Erdahl et al., 1994).

## The determination of cation transport

POPC vesicles containing Quin-2 or  $\text{La}^{3+}$  were utilized at a nominal phospholipid concentration of 1.0 or 1.5 mM, and at 25°C. The external medium contained 60 mM CsCl and 10 mM HEPES, pH 7.00, unless otherwise noted. The medium pH was adjusted with CsOH, which had been passed over Chelex 100 columns to remove contaminating cations (Erdahl et al., 1994). Valinomycin (Val) (0.5  $\mu\text{M}$ ) and carbonyl cyanide *m*-chlorophenylhydrazine (CCP) (5  $\mu\text{M}$ ) were normally present to maintain internal pH at the external value (Erdahl et al., 1995). However, one or both agents were omitted when we determined  $\text{H}^+/\text{La}^{3+}$  exchange ratios and the effects of an imposed membrane potential on transport kinetics, as further described below. Specific concentrations of ionophores and cations are given in the figure legends. Reactions were started by the addition of the carboxylic acid ionophore, after an initial 2–3-min period, which was allowed for the equilibration of internal and external pH.

The transport of  $\text{Ln}^{3+}$  was monitored by difference absorbance measurements that detect formation of the Quin-2:cation complex. An Aminco DW2a spectrophotometer operated in the dual-wavelength mode was employed, using the wavelength pair 267 versus 343 nm. The latter value is an isosbestic point in Quin-2/Quin-2: $\text{Ln}^{3+}$  difference spectra, which gave a difference extinction coefficient for the Quin-2: $\text{La}^{3+}$  complex of  $27,180 \pm 275 (\text{M}^{-1} \text{ cm}^{-1})$  ( $n = 5$ ), and similar values for other  $\text{Ln}^{3+}$ . The value specific to each cation was employed when relative rates of transport were determined. An Oriel no. 59800 bandpass filter was used between the cuvette and the beam scrambler-photomultiplier assembly in the spectrophotometer to prevent detection of the fluorescent light emitted by Quin-2 and A23187. Data were collected on disk with Unkel Scope software (Unkel Software, Lexington, MA).

## The determination of $\text{H}^+/\text{La}^{3+}$ exchange ratios

The stoichiometry of  $\text{H}^+/\text{La}^{3+}$  exchange was determined by simultaneous measurement of extravesicular pH and  $\text{La}^{3+}$  transport. Conditions were the same as described above, except that the external buffer concentration was reduced to 3 mM (HEPES only), and CCP or both Val and CCP were omitted, as specified in the figure legends. A Fisher Scientific AccupHast electrode and a Beckman model 4500 pH meter were employed, together with a strip chart recorder. The electrode was inserted into the cuvette, which was mounted in the open sample compartment of the dual-wavelength spectrophotometer, under darkened room conditions. To avoid disturbing the electrode by manual mixing, the magnetic stirring accessory provided by Aminco was operated throughout the experiment. The observed changes in external pH were calibrated by adding aliquots of a standard HCl solution in the absence of ionophore. This allowed the moles of  $\text{H}^+$  released from the vesicles during transport to be calculated at times selected from the continuous recordings of external pH. These values were plotted (as individual points) versus time, together with the transport progress curves, to reveal the exchange ratios.

## Analysis of transport data

External and internal methods were compared when  $\text{Ln}^{3+}$  transport was calibrated. For the external method, vesicles containing a known amount of

Quin-2 were lysed with 0.33% (w/v) of  $\text{Cs}^+$ -deoxycholate and then titrated with a standard cation solution under the conditions of interest. For the internal method, Quin-2 was titrated without lysing the vesicles, by including an excess of an appropriate ionophore in the system. Data obtained by the two methods were coincident, indicating that entrapment of Quin-2 and its complexes does not perturb their spectral properties.

To extract the initial rates of transport, early portions of the progress curves were fit to Eq. 1 by standard nonlinear least-squares methods:

$$A_T = A_0 + Bt + Ct^2 \quad (1)$$

In Eq. 1,  $A_T$  and  $A_0$  are the observed and the initial absorbance values, respectively;  $B$  is the initial rate;  $C$  is a correction factor for nonlinearity; and  $t$  is time. Rates are expressed in units of  $\mu\text{M/s}$  or  $\text{nM/s}$  of external cation transported into the vesicles. Transport selectivities are expressed as  $S$  values, defined by Eq. 2:

$$S_{\text{M}^{n+}} = \frac{\text{Initial rate of } \text{M}^{n+} \text{ transport}}{\text{Initial rate of } \text{Ca}^{2+} \text{ transport}} \quad (2)$$

When  $S$  is determined, an equal concentration of the cation in question is substituted for  $\text{Ca}^{2+}$ , with all other conditions held constant (Erdahl et al., 1996).

## RESULTS

### Transport selectivity and related properties

Fig. 2 shows that all commonly used  $\text{Ca}^{2+}$  ionophores transport a range of  $\text{Ln}^{3+}$  across the POPC vesicle membrane, and that marked differences exist in the rates of transport and the shapes of the progress curves, depending on the cation and ionophore considered. Initial rates were obtained from these data (Eq. 1), together with a value for  $\text{Ca}^{2+}$  transport under the same conditions (data not shown), and were utilized to calculate the selectivity values (Eq. 2) presented in Table 1. For 4-BrA23187 and ionomycin, the selectivity values are near 1 when the  $\text{Ln}^{3+}$  that are transported most rapidly are considered. With A23187,  $\text{Ca}^{2+}$  is transported more rapidly than any of the  $\text{Ln}^{3+}$ , but only by a factor of 3–5 in most cases. The absolute rates of  $\text{Ln}^{3+}$  transport span  $\sim 34$ -fold in the case of A23187 and 4-BrA23187 and  $\sim 4$ -fold in the case of ionomycin (Table 1). These findings show that transport of  $\text{Ln}^{3+}$  by  $\text{Ca}^{2+}$  ionophores is not a minor activity, but approaches the efficiency of  $\text{Ca}^{2+}$  transport under the conditions of Fig. 2. They also show that A23187 and 4-BrA23187 have substantial transport selectivity for individual  $\text{Ln}^{3+}$  cations, among the group investigated.

$\text{La}^{3+}$  was selected from the initial group of seven cations for most aspects of studies that follow. It is transported at a high efficiency by ionomycin, and is intermediate among the others when transported by A23187 and 4-BrA23187 (Fig. 2). The effect of  $\text{La}^{3+}$  concentration on initial rate is shown in Fig. 3. With A23187 and ionomycin, the initial rate decreases as the  $\text{La}^{3+}$  concentration is increased, whereas a modest increase is obtained with 4-BrA23187. Comparing these data to Fig. 2 suggests that  $\sim 8$ – $10 \mu\text{M}$  is an optimal concentration for  $\text{La}^{3+}$  transport catalyzed by

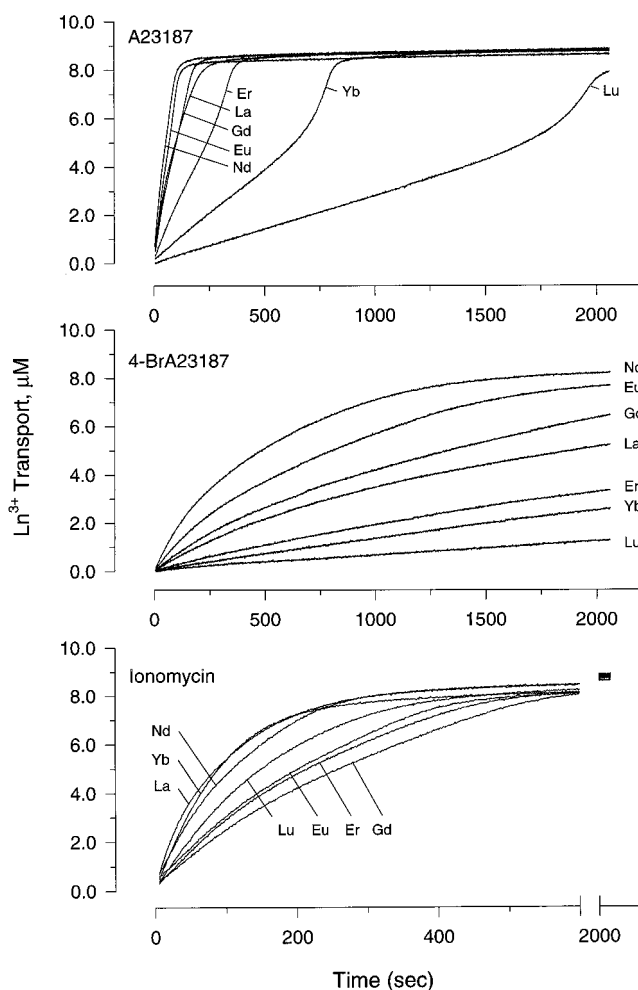


FIGURE 2 Transport of  $\text{Ln}^{3+}$  by  $\text{Ca}^{2+}$  ionophores. Experiments were conducted as described in Materials and Methods using POPC vesicles loaded with Quin-2. The nominal POPC concentration was 1.0 mM.  $\text{Ln}^{3+}$ , as perchlorates, were present at an initial concentration of  $9.0 \mu\text{M}$  in a medium that also contained 60 mM CsCl, 10 mM HEPES ( $\text{Cs}^+$ ), pH 7.00,  $0.5 \mu\text{M}$  Val, and  $5 \mu\text{M}$  CCP. At  $t = 0$ , transport of the indicated  $\text{Ln}^{3+}$  was initiated by addition of the following: (A) A23187 ( $1.2 \mu\text{M}$ ); (B) 4-BrA23187 ( $1.2 \mu\text{M}$ ); (C) ionomycin ( $1.5 \mu\text{M}$ ). Formation of the Quin-2: $\text{Ln}^{3+}$  complex within the vesicle lumen was monitored by dual wavelength spectroscopy, as described in Materials and Methods.

A23187 and ionomycin. This is because in Fig. 2, where the initial  $\text{La}^{3+}$  concentration was  $9 \mu\text{M}$ , the rate of transport decreases progressively as the process proceeds, even though little or no reverse reaction is occurring. Such behavior would be expected if the absolute rate were limited by the external  $\text{La}^{3+}$  concentration, because of a limiting formation of the transporting species at the outer membrane interface. Thus, at  $\text{La}^{3+}$  concentrations above (Fig. 3) and below (Fig. 2)  $\sim 9 \mu\text{M}$ , the rate of transport is diminished. The transport of  $\text{Zn}^{2+}$  and  $\text{Mn}^{2+}$  by A23187 and 4-BrA23187 is also characterized by an optimal cation concentration (Erdahl et al., 1996), whereas this is not true for  $\text{Ca}^{2+}$  transport, or for any of these divalent cations when transported by ionomycin (Erdahl et al., 1994, 1996).

TABLE 1  $\text{Ln}^{3+}$  transport by divalent cation ionophores

Ionophore	Cation							
	$\text{Ca}^{2+}$	$\text{La}^{3+}$	$\text{Nd}^{3+}$	$\text{Eu}^{3+}$	$\text{Gd}^{3+}$	$\text{Er}^{3+}$	$\text{Yb}^{3+}$	$\text{Lu}^{3+}$
A23187								
Rate	364	89.7	117	85.2	66.5	22.9	8.00	3.50
Selectivity	1.00	0.25	0.32	0.23	0.18	0.06	0.02	0.01
4-BrA23187								
Rate	16.4	5.30	20.3	11.9	7.20	2.30	1.40	0.60
Selectivity	1.00	0.32	1.24	0.72	0.44	0.14	0.08	0.04
ionomycin								
Rate	70.1	97.3	55.3	27.6	24.2	29.3	68.8	40.0
Selectivity	1.00	1.39	0.79	0.39	0.35	0.42	0.98	0.57

Initial rates of  $\text{Ln}^{3+}$  transport (in units of nM/s) were obtained from the data in Fig. 2, using Eq. 1, as described in Materials and Methods. The uncertainty in these values is  $\pm 5\%$  (Erdahl et al., 1994). Selectivity ( $S$  values) was calculated according to Eq. 2, using a value for the initial rate of  $\text{Ca}^{2+}$  transport determined under the same conditions (see legend to Fig. 2).

### Stoichiometry of the transporting species and mode of transport

If it is assumed that transmembrane diffusion of the transporting species is the slowest step in the mechanism (Kolber et al., 1981), the stoichiometry of the species can be obtained, as the slope, from plots of log initial rate of transport versus log of the ionophore concentration (Blau et al., 1984, 1988; Erdahl et al., 1994, 1996). As seen in Fig. 4 and Table 2, these values are somewhat greater than 2 in the case of A23187 and 4-BrA23187, and greater than 1 with ionomycin, when determined at a  $\text{La}^{3+}$  concentration of  $15 \mu\text{M}$ . At  $250 \mu\text{M}$   $\text{La}^{3+}$ , the values for A23187 and ionomycin decrease slightly, more nearly approaching 2 and 1, respectively. These data indicate a predominant stoichiometry of

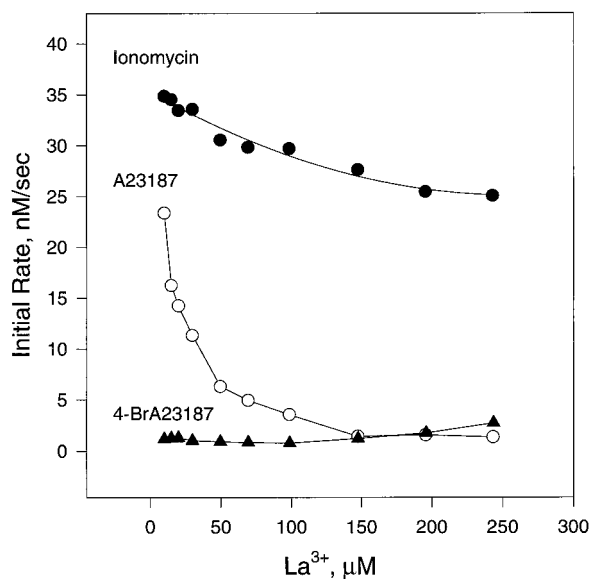


FIGURE 3 Effect of cation concentration on the initial rate of  $\text{La}^{3+}$  transport. Conditions were the same as described in the legend to Fig. 1, except that the ionophore concentration was  $1.0 \mu\text{M}$  in all cases and the external  $\text{La}^{3+}$  concentration was varied as shown.



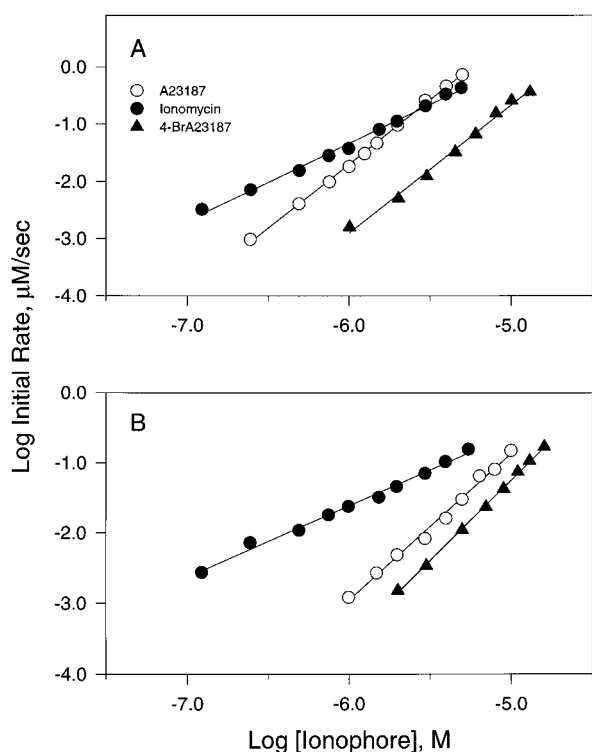


FIGURE 4 Relationship between the initial rate of  $\text{La}^{3+}$  transport and ionophore concentration. Experiments were conducted as described in Materials and Methods and the legend to Fig. 2, using the indicated concentrations of ionophores. The  $\text{La}^{3+}$  concentration was 15  $\mu\text{M}$  (A) or 250  $\mu\text{M}$  (B). Each set of data points was fit to a linear equation, to obtain the slopes, which are presented separately in Table 2.

2:1 (ionophore:cation) (A23187 and 4-BrA23187) and 1:1 (ionomycin), and that species of higher stoichiometry are also contributing.

In the fully ionized state, A23187 and 4-BrA23187 are monobasic compounds, whereas ionomycin is dibasic (Fig. 1; Toepilitz et al., 1979; Debono et al., 1981). Accordingly, 2:1 complexes (A23187 and 4-BrA23187) and 1:1 complexes (ionomycin) containing  $\text{La}^{3+}$  carry a charge of 1+. Thus it seemed possible that  $\text{La}^{3+}$  is transported by an electrogenic mechanism when Val plus CCP is present to collapse the resulting membrane potential. To investigate this possibility, the effect of an imposed potential was

TABLE 2 Stoichiometry of the transporting species: slope of the log-log plots

$\text{La}^{3+}$ , Concentration	Slope		
	A23187	4-BrA23187	Ionomycin
$\text{La}^{3+}$ , 15 $\mu\text{M}^*$	2.24	2.24	1.39
$\text{La}^{3+}$ , 250 $\mu\text{M}^*$	2.09	2.30	1.02
$\text{La}^{3+}$ , 17 mM*	3.02	3.07	1.08
$\text{Lu}^{3+}$ , 15 $\mu\text{M}^\#$	3.01	2.80	N.D.

\*Values were obtained from data sets like those shown in Fig. 4, A (15  $\mu\text{M}$ ) and B (250  $\mu\text{M}$ ), or Fig. 8 (17 mM).

<sup>#</sup>Values were obtained from experiments like those shown in Fig. 2, except that the concentration of  $\text{Lu}^{3+}$  was 15  $\mu\text{M}$ .

determined using vesicles containing a high internal  $\text{K}^+$  concentration and an external medium containing  $\text{Na}^+$ . In that system, when Val and CCP are excluded, all three compounds remain active as  $\text{La}^{3+}$  ionophores (Fig. 5). This shows that electroneutral mechanisms are operating when no potential is imposed. However, in each case, when Val was also present, but CCP was not present, the rate of  $\text{La}^{3+}$  transport was accelerated notably (Fig. 5). Measurements carried out with a tetraphenylphosphonium cation ( $\text{TPP}^+$ ) electrode (Kamo et al., 1979; Erdahl et al., 1994) showed that the presence of Val resulted in a membrane potential of  $\sim 160$  mV, inside negative, that is maintained throughout the period of  $\text{La}^{3+}$  accumulation (data not shown). Accordingly, it appeared that  $\text{La}^{3+}$  might be transported through a mixed mode mechanism when a membrane potential of the appropriate orientation is present.

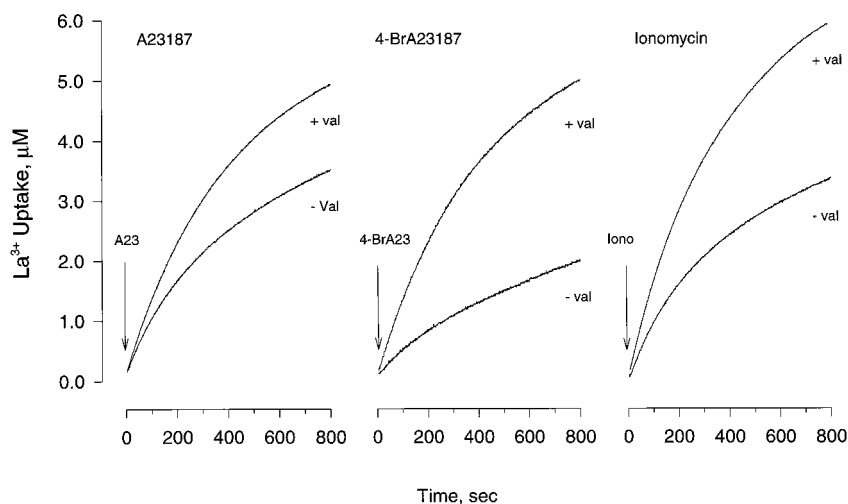
The mode of transport was further examined by determining the ratio of  $\text{H}^+$  released per  $\text{La}^{3+}$  accumulated under several conditions. When the medium and vesicles are analogous to those employed for Figs. 2–4, three  $\text{H}^+$  are released per  $\text{La}^{3+}$  accumulated when Val and CCP are absent, regardless of which carboxylic acid ionophore is considered (Fig. 6). With  $\text{K}^+$ -containing vesicles placed in the  $\text{Na}^+$ -containing medium, the ratio remained at 3 when A23187 or ionomycin was employed, regardless of whether or not a membrane potential was imposed by use of Val (Fig. 7, A and C). With 4-BrA23187, a ratio of 3 is again obtained when Val is absent, but the value is reduced in the presence of Val (Fig. 7 B). Thus it is seen that 2:1 complexes between A23187 or 4-BrA23187 and  $\text{La}^{3+}$ , and a 1:1 complex between ionomycin and  $\text{La}^{3+}$ , can affect a  $3\text{H}^+/\text{La}^{3+}$  exchange (Fig. 6); that transport catalyzed by all three ionophores is accelerated by membrane potential (Fig. 5); and, in one case (4-BrA23187), that the accelerated transport is accompanied by a lowered stoichiometry of  $\text{H}^+/\text{La}^{3+}$  exchange (Fig. 7).

### $\text{La}^{3+}$ release from $\text{La}^{3+}$ -loaded vesicles

When the direction of  $\text{La}^{3+}$  transport is reversed by using  $\text{La}^{3+}$ -loaded vesicles, with Quin-2 present in the external medium, the progress curves obtained with A23187 and 4-BrA23187 display a sigmoidal characteristic (Fig. 8 A). This property is also seen during  $\text{Yb}^{3+}$  and  $\text{Lu}^{3+}$  transport into the vesicles catalyzed by A23187 (Fig. 2). In contrast, ionomycin produces a hyperbolic-like progress curve when transporting  $\text{La}^{3+}$  in either direction (Figs. 2 and 8 A). The  $\text{La}^{3+}$  concentration near the membrane interface where the transporting species forms is a factor that varies dramatically between the accumulation and release experiments. For the former (Fig. 2) the value was  $\sim 9$   $\mu\text{M}$ , whereas for the latter (Fig. 8 A) it was  $\sim 17$  mM, ignoring cation-membrane interactions and other surface-related factors.

Given the complex shape of the  $\text{La}^{3+}$  release curves, initial rate values obtained as a function of ionophore concentration show more scatter than is apparent when trans-

FIGURE 5 Influence of membrane potential on  $\text{La}^{3+}$  transport. Experiments were performed as described in Materials and Methods, except that the vesicles were formed in a medium containing 10 mM HEPES ( $\text{K}^+$ ), pH 7.00, 5 mM Quin-2 ( $\text{K}^+$ ) and 100 mM KCl. These conditions reduced the internal Quin-2 concentration to 3.9 mM, and gave an internal  $\text{K}^+$  concentration of 125 mM. The external medium contained 10 mM HEPES ( $\text{Na}^+$ ), pH 7.00, 100 mM NaCl, 15  $\mu\text{M}$   $\text{La}(\text{ClO}_4)_3$  and vesicles at 1.5 mM POPC. Where indicated, Val was present at 0.5  $\mu\text{M}$ , and was added before the indicated carboxylic acid ionophore, which was used at 1.0  $\mu\text{M}$  (A23187 and ionomycin) or 3.2  $\mu\text{M}$  (4-BrA23187). CCP was not present during any of the experiments.



port occurs in the opposite direction. Nevertheless, values of reasonable accuracy could be obtained, and are shown as a plot of log initial rate of transport versus log ionophore concentration (Fig. 8 *B*) for comparison to Fig. 4. For A23187 and 4-BrA23187, the slopes were  $\sim 3$ , clearly higher than the values obtained for transport in the opposite direction (Table 2). In contrast, the value for ionomycin is 1.08, which is close to the value obtained during uptake at 250  $\mu\text{M}$   $\text{La}^{3+}$  (Table 2). Slopes were also obtained for the transport of 15  $\mu\text{M}$   $\text{Lu}^{3+}$  into vesicles by A23187 and 4-BrA23187, and were comparable to those obtained from Fig. 8 *B* in both cases (Table 2).

During  $\text{La}^{3+}$  release from  $\text{La}^{3+}$ -loaded vesicles, transport via a species carrying a net positive charge would produce a membrane potential oriented inside negative, which would be amenable to detection by the  $\text{TPP}^+$  electrode technique (Erdahl et al., 1994). Measurements of potential under the conditions of Fig. 8 *A*, but with Val and CCP absent, were negative at a detection limit of  $\sim 50$  mV (data not shown).

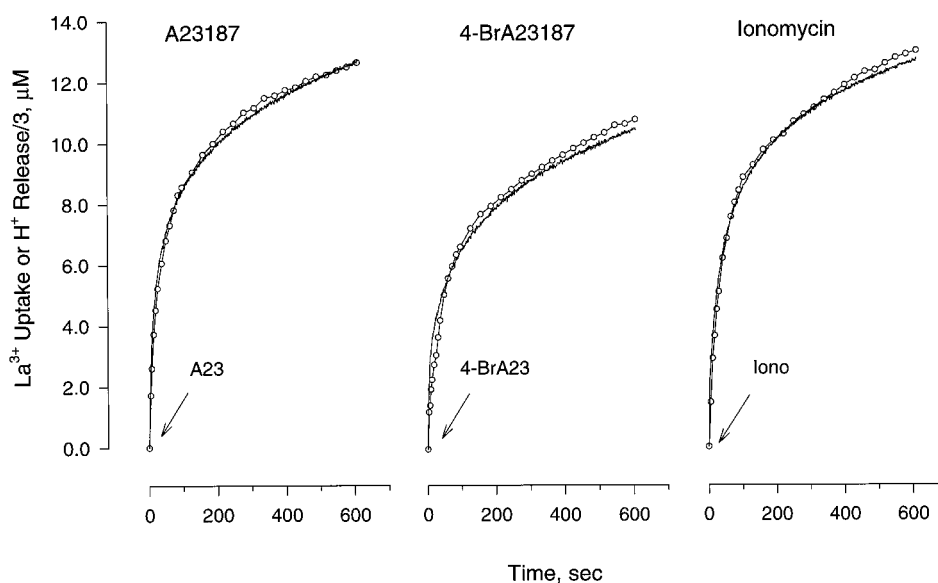
Thus  $\text{La}^{3+}$  release catalyzed by all three ionophores occurs through an electroneutral mechanism.

## DISCUSSION

### The predominant mechanism of $\text{La}^{3+}$ transport

This is the first study that allows ionophore-catalyzed  $\text{Ln}^{3+}$  transport to be evaluated mechanistically and in terms of specificity. The results indicate that  $\text{La}^{3+}$  transport occurs primarily as an electroneutral process, through mixed complexes that contain a single  $\text{OH}^-$ , when the cation concentration is within the range of 9–250  $\mu\text{M}$ . This is shown by the observed  $\text{H}^+/\text{La}^{3+}$  exchange ratios of 3 (Fig. 6), together with the stoichiometries of the transporting species (Fig. 4 and Table 2), as follows: A23187 and 4-BrA23187 are monocarboxylic acids (Fig. 1) that complex cations as the carboxylate anion (Smith et al., 1976; Chapman et al., 1987). After transport of a single  $\text{La}^{3+}$  as the 2:1 complex

FIGURE 6 Stoichiometry of  $\text{H}^+/\text{La}^{3+}$  exchange in the absence of membrane potential. The vesicles utilized were prepared in the medium described in Materials and Methods and were present at a nominal POPC concentration of 1.5 mM. The external medium contained 3 mM HEPES ( $\text{Cs}^+$ ), pH (initial) 7.00, and 21  $\mu\text{M}$   $\text{La}(\text{ClO}_4)_3$ . Val and CCP were not present.  $\text{La}^{3+}$  accumulation and external pH were determined simultaneously, and calibrated, as described in Materials and Methods. The continuous traces are  $\text{La}^{3+}$  accumulation, in units of  $\mu\text{M}$  external concentration. The open circles show  $\text{H}^+$  release, divided by 3, in the same units. Reactions were started by addition of the indicated carboxylic acid ionophore at 5  $\mu\text{M}$  (A23187 and ionomycin) or 14  $\mu\text{M}$  (4-BrA23187).



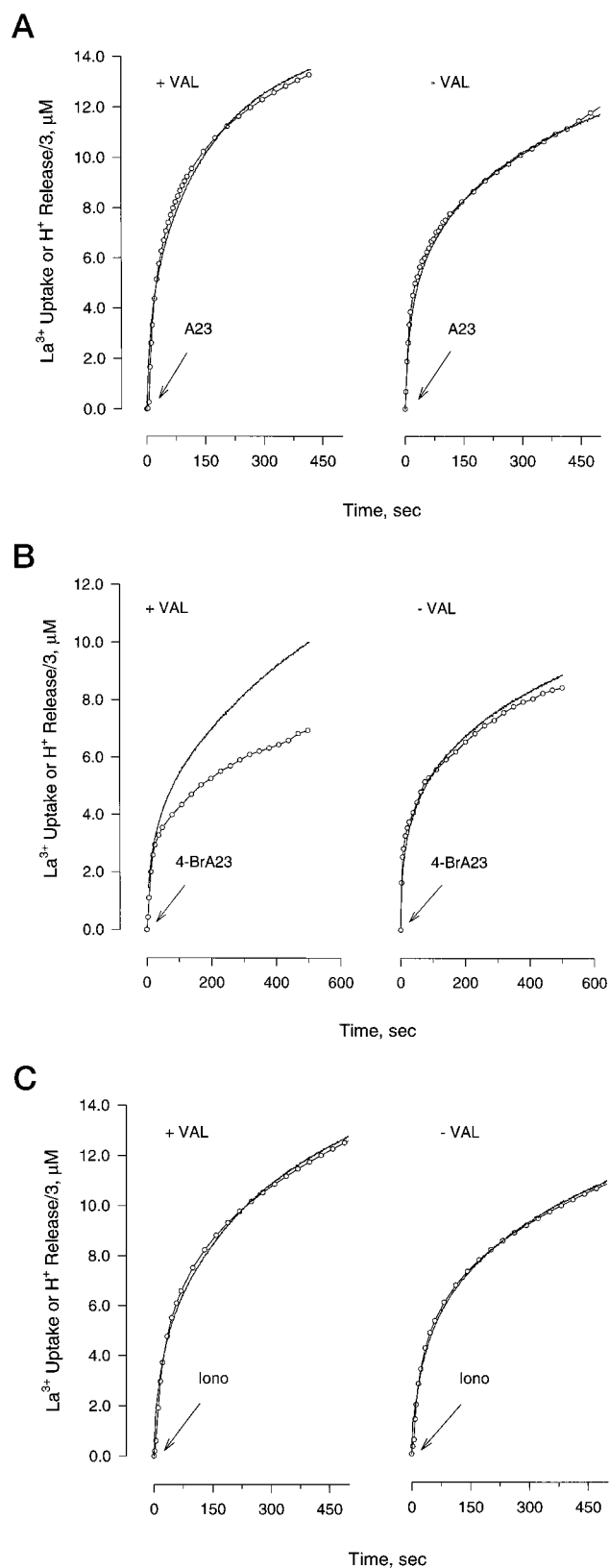


FIGURE 7 Stoichiometry of  $\text{H}^+/\text{La}^{3+}$  exchange in the presence of membrane potential. Experiments were conducted as described in the legend to Fig. 6, using  $\text{Na}^+$ -HEPES rather than  $\text{Cs}^+$ -HEPES in the external medium. In addition, the vesicles were formed in a medium containing 5 mM Quin-2 ( $\text{K}^+$ ) and 20 mM KCl. Reactions were started by the addition of 5 μM A23187 or ionomycin (A and C, respectively), or 14 μM 4-BrA23187 (B).

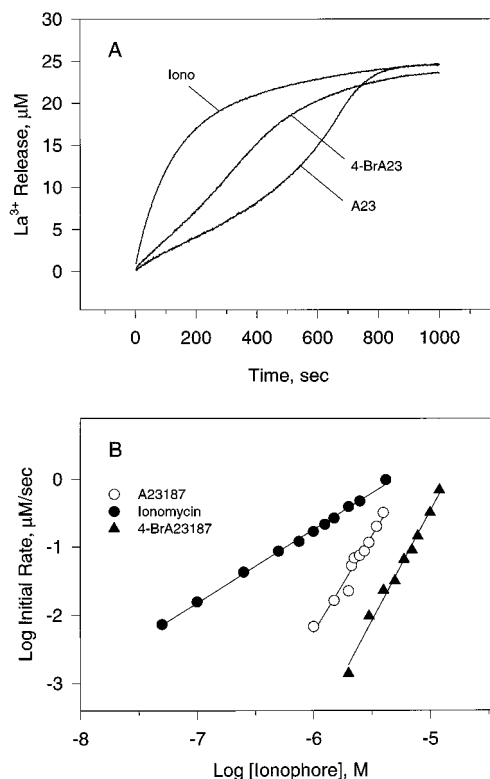


FIGURE 8  $\text{La}^{3+}$  release from  $\text{La}^{3+}$ -loaded vesicles. Vesicles were prepared in a medium containing 5 mM  $\text{LaCl}_3$  and 10 mM 2-(*N*-morpholino)ethanesulfonic acid ( $\text{Cs}^+$ ), pH 6.00, as further described in Materials and Methods. The external medium contained 25 μM Quin-2 ( $\text{Cs}^+$ ), 10 mM HEPES ( $\text{Cs}^+$ ), pH 7.00, 10 mM  $\text{CsCl}$ , 0.5 μM Val, 5 μM CCP, and vesicles at a nominal POPC concentration of 1.0 mM. (A)  $\text{La}^{3+}$  release was initiated at  $t = 0$  by the addition of 2.0 μM A23187, 5.0 μM 4-BrA23187, or 1.0 μM ionomycin, as indicated. (B) Conditions were the same as described for A, except that the ionophore concentrations were varied as shown.

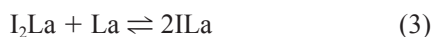
(ionophore:cation), only two  $\text{H}^+$  would be moved to the opposite side of the membrane upon return of the protonated, uncomplexed molecules. Similarly, ionomycin is a monocarboxylic acid but contains an enolized  $\beta$ -diketone moiety (Fig. 1) that is also ionized in 1:1 cation complexes (Toepfilitz et al., 1979; Stiles et al., 1991). Accordingly, 1:1 complexes of this ionophore can also produce a  $2\text{H}^+/\text{cation}$  exchange, but not an exchange of higher stoichiometry. In both cases, the third  $\text{H}^+$  can be accounted for only by the presence of an  $\text{OH}^-$  in the transporting species. Upon entering a vesicle together with  $\text{La}^{3+}$ , this  $\text{OH}^-$  becomes equivalent to a  $\text{H}^+$  that is released, with respect to measured values of  $\text{H}^+/\text{La}^{3+}$  exchange. In addition, the presence of  $\text{OH}^-$  in the species that transport  $\text{La}^{3+}$  provides for a net charge of zero on the complexes. This property is also required in an electroneutral mechanism. In the case of A23187, transport of  $\text{Ln}^{3+}$  through mixed complexes con-

When present, 0.5 μM Val was added 1 min before the carboxylic acid ionophore to generate a membrane potential with an inside-negative orientation. CCP was not present during any of the experiments.

taining  $\text{OH}^-$  was predicted from solution equilibrium studies which showed that the requisite complexes exist in a solvent (80% methanol/water) that mimics the dielectric environment at a membrane interface (Chapman et al., 1990b).

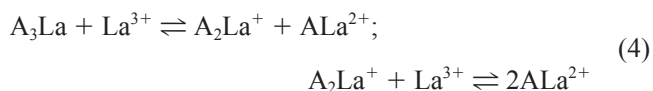
### $\text{Ln}^{3+}$ transport via other species

Aspects of the data also indicate that a fraction of  $\text{La}^{3+}$  transport occurs through complexes of higher stoichiometry. Within the cation concentration range of 9–250  $\mu\text{M}$ , this is shown by slopes of the log initial rate versus log ionophore concentration plots, which generally exceed 2 for A23187 and 4-BrA23187, or 1 for ionomycin (Table 2). Presumably, the higher order complexes are  $(\text{A23187 or 4-BrA23187})_3\text{La}$  and  $\text{H}(\text{ionomycin})_2\text{La}$  because these are also neutral species and could produce a  $3\text{H}^+/\text{La}^{3+}$  exchange. These species have not been detected by solution equilibrium methods; however, the inverse relationships between  $\text{La}^{3+}$  concentration, slopes (Table 2), and rates of transport (Fig. 3) support their involvement as follows. Considering ionomycin first, a complex containing two ionophore molecules would be subject to comproportionation with a rising  $\text{La}^{3+}$  concentration, as illustrated by Eq. 4 (protonation state and net charge not designated):



As a consequence, the fraction of transport occurring via the 2:1 complex is expected to decrease as the  $\text{La}^{3+}$  concentration rises, explaining the inverse relationship between slope and cation concentration (Table 2). Since in general, the species of 2:1 and 1:1 stoichiometry would have different transmembrane diffusion constants, the rate of transport would change with the extent of comproportionation. Thus the inverse relationship between rate of transport and  $\text{La}^{3+}$  concentration, while the ionomycin concentration is held constant (Fig. 3), can also be explained if both 2:1 and 1:1 species are involved.

With A23187 and 4-BrA23187, the comproportionation equilibria applicable to a 3:1 complex are as follows;



Regarding A23187, when these reactions are considered together with Fig. 3 and Table 2, the indications are that the  $\text{A}_3\text{La}$  species exists, but is not prevalent, even at 15  $\mu\text{M}$   $\text{La}^{3+}$  (slope only slightly greater than 2). The marked loss of transport activity with increasing  $\text{La}^{3+}$  concentration (Fig. 3), together with retention of a predominant 2:1 stoichiometry at 250  $\mu\text{M}$   $\text{La}^{3+}$  (Table 2), is taken to indicate that the 1:1 complex, arising ultimately from comproportionation (Eq. 4), is not a transporting species. This interpretation is consistent with the relatively high coordination number of  $\text{La}^{3+}$  (8–10), together with the much lower number of liganding atoms available in one molecule of A23187

(three). Thus in a 1:1 complex, even if one or two  $\text{OH}^-$  were included, there would still be several coordination sites available to interact with  $\text{H}_2\text{O}$  and thereby limit membrane permeability.

With 4-BrA23187, transport occurs relatively slowly across the entire  $\text{La}^{3+}$  concentration region considered in Fig. 3, yet a mixture of 2:1 and 3:1 species is contributing at 15 and 250  $\mu\text{M}$   $\text{La}^{3+}$  (slopes greater than 2). The low transport activity seen near 15  $\mu\text{M}$   $\text{La}^{3+}$ , in comparison to the activity of A23187, can be explained by weaker inter-ligand hydrogen bonds between the two ionophore molecules of the 2:1 complex (Erdahl et al., 1996). This, in effect, shifts the comproportionation equilibria to the right at any given  $\text{La}^{3+}$  concentration (relative to A23187), lowering the prevalence of 2:1 species, and thereby diminishing the rate of transport.

The above interpretations explain most of the data relating the concentrations of  $\text{Ln}^{3+}$  and ionophore to the kinetics of transport. There is an exception, however, in that it is not clear how the  $(\text{ionophore})_3\text{Ln}$  species that contribute to  $\text{Ln}^{3+}$  transport by A23187 and 4-BrA23187 are formed. These species predominate in transporting  $\text{La}^{3+}$  when the cation concentration is 17 mM (Table 2), which is surprising, given solution equilibrium studies which show that the 1:1 association constant for  $\text{A}^-$  and  $\text{La}^{3+}$  is  $\sim 10^6 \text{ M}^{-1}$  at pH 7 (Chapman et al., 1990b), and that the second stepwise stability constant for formation of  $(\text{ionophore})_2\text{M}$  species generally exceeds the first value by only a fewfold (Tissier et al., 1993). Accordingly, the  $(\text{ionophore})_3\text{La}$  species form and transport  $\text{La}^{3+}$  when the great majority of ionophore is expected to exist as the 1:1 complex. A similar relationship was seen with  $\text{Ca}^{2+}$  transport mediated by A23187, which attains a maximum rate at cation concentrations where the 1:1 complex predominates (Erdahl et al., 1994). Such a concentration dependence is observed, even though it is the  $(\text{A23187})_2\text{Ca}$  complex that transports  $\text{Ca}^{2+}$  (Erdahl et al., 1994, 1995).

It seems possible that membrane-associated cation is involved in forming the higher order species when aqueous phase solution conditions favor a 1:1 complex. This is suggested by the increasing prevalence of 3:1 complexes as the aqueous phase cation concentration is increased (Table 2), together with the relatively high affinity of phosphatidylcholine membranes for lanthanide cations (Lehrmann et al., 1994). Regardless of how these complexes are formed, their occurrence at high cation concentrations provides an explanation for the sigmoid-like progress curves that were obtained in several experiments. This behavior is clearly seen in Fig. 8A, for example, for  $\text{La}^{3+}$  release catalyzed by A23187. The acceleration of transport that is seen as the vesicles become depleted of  $\text{La}^{3+}$  may reflect a progressive shift from transport via the 3:1 complex to a more efficient transport via a 2:1 mixed complex containing  $\text{OH}^-$ . The same interpretation can account for the sigmoid-like progress curves obtained with A23187 transporting  $\text{Lu}^{3+}$  and  $\text{Yb}^{3+}$  into Quin-2-loaded vesicles (Fig. 2). Regarding those data, it is interesting to note that the apparent shift in



the predominant transporting species occurs at a much higher free cation concentration with  $\text{La}^{3+}$  (several mM in Fig. 8 A), compared to  $\text{Lu}^{3+}$  and  $\text{Yb}^{3+}$  (several  $\mu\text{M}$  in Fig. 2). It seems possible that this difference might be exploited to obtain a separation of specific  $\text{Ln}^{3+}$  from mixtures.

### Influence of membrane potential and the specificity of transport

All three ionophores transport  $\text{La}^{3+}$  more rapidly when the direction is toward the negative side of an imposed membrane potential (Fig. 5). Nevertheless, with A23187 and ionomycin, three  $\text{H}^+$  are exchanged for each  $\text{La}^{3+}$  under all conditions examined. These include conditions where a potential would be manifest if it formed (Figs. 6 and 7, Val absent), and conditions where a substantial potential has been imposed (Fig. 7, Val present). Accordingly, with A23187 and ionomycin, the effects of an imposed potential do not reflect a significant fraction of transport occurring through an electrogenic mechanism.

In contrast, with 4-BrA23187, an imposed potential lowers the ratio of  $\text{H}^+/\text{La}^{3+}$  exchange (Fig. 7), indicating that an electrogenic mechanism is operating and is responsible for a sizable fraction of the total activity. Delocalization of positive charge in the species  $(4\text{-BrA23187})_2\text{La}^+$ , because of inductive/electronic effects of the bromine substituents, probably accounts for the electrogenic capability. In addition, the bromine substituents may increase hydrophobicity because an analogous substitution has that effect with La-salocid A (Westley, 1983). Because comproportionation will greatly reduce the steady-state level of  $(4\text{-BrA23187})_2\text{La}^+$  when the free  $\text{La}^{3+}$  concentration is high (Eq. 4), there is no conflict between the observation of a partially electrogenic mechanism at low  $\text{La}^{3+}$  and the absence of potential formation during  $\text{La}^{3+}$  release from  $\text{La}^{3+}$ -loaded vesicles.

Imposed potentials also accelerate the transport of  $\text{Ca}^{2+}$  by these ionophores, although the effects are smaller than with  $\text{La}^{3+}$ , and there is no indication of an electrogenic component with any of the compounds (Erdahl et al., 1994). Effects of membrane potential on rate, when the transport mode is electroneutral, have been attributed to uncatalyzed  $\text{H}^+$  diffusion into the vesicles. Under that proposal, the resulting decrease in luminal pH accelerates transport by altering the distribution of uncomplexed ionophore molecules across the membrane, and by favoring formation of the protonated form after transport and release of the cation (Erdahl et al., 1994, 1995). Because the constants of  $\text{Ca}^{2+}$  and  $\text{La}^{3+}$  adsorption to phosphatidylcholine bilayers are  $10\text{--}20\text{ M}^{-1}$  and  $4.1 \times 10^3\text{ M}^{-1}$ , respectively (Lehrmann et al., 1994), surface charge and headgroup effects arising from the binding of either cation will differ (Tocanne et al., 1990). These factors may alter uncatalyzed  $\text{H}^+$  diffusion and account for the larger effect of an imposed potential on the rate of  $\text{La}^{3+}$  transport.

The comparable activities for transport of  $\text{Ca}^{2+}$  and several  $\text{Ln}^{3+}$  are noteworthy regarding the use of these iono-

phores as research tools, and in terms of factors that establish their transport selectivity. In the former area,  $\text{Ca}^{2+}$  transport rises as the cation concentration is increased above  $9\text{ }\mu\text{M}$  (Erdahl et al., 1994, 1996), whereas  $\text{La}^{3+}$  transport remains essentially constant or declines (Fig. 3). Accordingly,  $S$  values, as defined by Eq. 2, would be smaller if determined at higher cation levels but would perhaps be larger, or less affected, at lower levels. Thus, when ionophores are used to manipulate cell  $\text{Ca}^{2+}$  while  $\text{Ln}^{3+}$  are present to inhibit ion-conducting channels, transport of the latter into cells and between subcellular compartments is probable.

The transport selectivity results can be related to solution chemical properties only in the case of A23187, because there are insufficient data for the others. In solution, 1:1 complexes between A23187 and the  $\text{Ln}^{3+}$  are 160–800-fold more stable than the corresponding  $\text{Ca}^{2+}$  complex and follow the order  $\text{Lu}^{3+} > \text{Yb}^{3+} > \text{Eu}^{3+} > \text{Er}^{3+} > \text{Gd}^{3+} > \text{Nd}^{3+} > \text{La}^{3+}$  (Chapman et al., 1990b). Although the relatively high stability of  $\text{ALn}^{2+}$  helps to explain an efficient transport at low  $\text{Ln}^{3+}$  concentrations, the stability sequence is similar to the transport sequence in reverse (Table 1). In addition, the stability constants span only  $\sim 5$ -fold (Chapman et al., 1990b), whereas transport selectivity spans  $\sim 34$ -fold (Table 2). These patterns reinforce other results which indicate that the stability of 1:1 complexes is not a factor of primary importance in determining the transport selectivity of this ionophore (Erdahl et al., 1996). Complexation equilibria and kinetics, in association with  $\text{OH}^-$ , and unidentified reactions that form transporting species from membrane associated ionophore are apparently of greater importance, but are less well understood.

### ENDNOTES

1. (The concentration of solutes in vesicles prepared by freeze-thaw extrusion exceeds their concentration in the formation medium by several fold under some circumstances (Chapman et al., 1990a, 1991). This concentrating effect is thought to be driven by freezing, which tends to exclude solutes from the growing ice phase, while increasing their concentration in the remaining liquid phase, were the vesicles are located (Chapman et al., 1990a, 1991).)

2. (The association constants for Quin-2 and  $\text{Ln}^{3+}$  are on the order of  $10^{12}\text{ M}^{-1}$  (Chapman et al., 1990a, 1991), whereas they are  $\sim 10^6\text{ M}^{-1}$  for ionophore complexes involving these cations (Chapman et al., 1990b). Because the total Quin-2 entrapped substantially exceeds the total  $\text{Ln}^{3+}$  transported into the vesicles (factor of  $\sim 2.5$ ), the internal concentration of free  $\text{Ln}^{3+}$  during accumulation will remain far below the range required for a significant reverse reaction ( $\text{Ln}^{3+}$  release).)

3. (Assuming the vesicles to be spherical condensers with an outer diameter of 70 nm and a bilayer thickness of 2.9 nm (Chapman et al., 1990a), their electrical capacitance ( $C$ ) can be calculated from Eq. E-1:

$$C = \frac{1.11 \times 1.0^{-12} \epsilon R_o R_i}{R_o - R_i} \quad (\text{E-1})$$

In this expression,  $\epsilon$  is the membrane dielectric constant,  $R_o$  and  $R_i$  are the outer and inner radii of the vesicles (in cm), and  $C$  is obtained in farads (F). At  $\epsilon = 2.5$  (Wrigglesworth et al., 1990), the calculated capacitance of a single vesicle is  $1.08 \times 10^{-16}\text{ F}$ , or  $0.70\text{ }\mu\text{F}/\text{cm}^2$ . The latter value approximates those that have been measured ( $\sim 0.6\text{ }\mu\text{F}/\text{cm}^2$ ; e.g., Montal,

1970). Using the calculated value, other vesicle parameters (Chapman et al., 1990a), and the amount of  $\text{La}^{3+}$  entrapped ( $\sim 1400/\text{vesicle}$ ), it can be shown that transport of a single charge across the membrane of one vesicle will create a membrane potential of  $\sim 1.5$  mV, and that the release of 2–3% of the entrapped  $\text{La}^{3+}$  via complexes that carry a net charge of 1+ would produce a membrane potential above the detection limit of the TPP<sup>+</sup> electrode method, at the vesicle concentration used to obtain Fig. 8.)

4. (Regarding this discussion of comproportionation equilibria, there is no intent to imply that the species considered are formed de novo by any particular reaction mechanism.)

5. (To illustrate potential levels of  $\text{Ln}^{3+}$ -A23187 complexes, species distribution calculations (Perrin et al., 1967) were carried out for systems with the following compositions: pH 7;  $[\text{A23187}]_{\text{tot}} = 1.2 \mu\text{M}$ ;  $[\text{Ln}^{3+}]_{\text{tot}} = 15 \mu\text{M}$ , 250  $\mu\text{M}$ , or 17 mM. Based on previous studies (Tissier et al., 1985, 1993; Chapman et al., 1990b),  $10^6 \text{ M}^{-1}$  was used as the conditional formation constant (approximate) of the first and second stepwise complex formation reactions (analogous to Eqs. 5 and 6). These constants account for the protonation and hydrolysis side reactions involving the metal ion, ionophore, and the complex, but are valid only at a given pH. The calculations showed that concentrations of  $\text{A}_2\text{Ln}'$  species, where  $[\text{A}_2\text{Ln}'] = [\text{A}_2\text{Ln}^{+}] + [\text{A}_2\text{Ln}(\text{OH})]$ , and the percentage of total ionophore that would not be complexed are as follows:  $[\text{Ln}^{3+}]_{\text{tot}} = 15 \mu\text{M}$ ,  $[\text{A}_2\text{Ln}'] = 7.0 \times 10^{-8} \text{ M}$  (5.9%);  $[\text{Ln}^{3+}]_{\text{tot}} = 250 \mu\text{M}$ ,  $[\text{A}_2\text{Ln}'] = 5.6 \times 10^{-9} \text{ M}$  (0.40%);  $[\text{Ln}^{3+}]_{\text{tot}} = 17 \text{ mM}$ ,  $[\text{A}_2\text{Ln}'] = 8.5 \times 10^{-11} \text{ M}$  (0.006%). Levels of putative  $\text{A}_3\text{Ln}$  complexes could not be estimated because no information is available on their stability. However, these levels would be lower than those of 2:1 complexes in all cases.)

This research was supported by U.S. Public Health Service grants HL 49181 and HL 49182 from the National Institutes of Health, National Heart, Lung and Blood Institute.

## REFERENCES

- Albin, M., B. M. Cader, and Horrocks, Jr. 1984. Lanthanide complexes of Ionophore. 2. Spectroscopic characterization of lanthanide (III) ion binding to lasalocid A and A23187. *Inorg. Chem.* 23:3045–3050.
- Amellel, M., and Y. Landry. 1983. Lanthanides are transported by ionophore A23187 and mimic calcium in the histamine release process. *Br. J. Pharmacol.* 80:365–370.
- Bartlett, G. R. 1959. Phosphorous assay in column chromatography. *J. Biol. Chem.* 234:466–468.
- Blau, L., R. B. Stern, and R. Bittman. 1984. The stoichiometry of A23187- and X537A-mediated calcium ion transport across lipid bilayers. *Biochim. Biophys. Acta.* 778:219–223.
- Blau, L., and G. Weissmann. 1988. Transmembrane calcium movements mediated by ionomycin and phosphatidate in liposomes with fura 2 entrapped. *Biochemistry.* 27:5661–5666.
- Chapman, C. J., W. L. Erdahl, R. W. Taylor, and D. R. Pfeiffer. 1990a. Factors affecting solute entrapment in POPC vesicles prepared by the freeze-thaw extrusion method. *Chem. Phys. Lipids.* 55:73–83.
- Chapman, C. J., W. L. Erdahl, R. W. Taylor, and D. R. Pfeiffer. 1991. Effect of solute concentration on the entrapment of solutes in phospholipid vesicles prepared by freeze-thaw extrusion. *Chem. Phys. Lipids.* 60:201–208.
- Chapman, C. J., A. K. Puri, R. W. Taylor, and D. R. Pfeiffer. 1987. Equilibria between ionophore A23187 and divalent cations: the stability of 1:1 complexes in solutions of 80% methanol/water. *Biochemistry.* 26:5009–5018.
- Chapman, C. J., A. K. Puri, R. W. Taylor, and D. R. Pfeiffer. 1990b. General features in the stoichiometry and stability of ionophore A23187-cation complexes in homogenous solution. *Arch. Biochem. Biophys.* 281:44–57.
- Debono, M., R. M. Molloy, D. E. Dorman, J. W. Paschal, D. F. Babcock, C. M. Deber, and D. R. Pfeiffer. 1981. Synthesis and characterization of halogenated derivatives of ionophore A23187: enhanced  $\text{Ca}^{2+}$  transport specificity by the 4-bromo derivative. *Biochemistry.* 20:6865–6872.
- Erdahl, W. L., C. J. Chapman, R. W. Taylor, and D. R. Pfeiffer. 1994.  $\text{Ca}^{2+}$  transport properties of ionophores A23187, ionomycin, and 4-BrA23187 in a well defined system. *Biophys. J.* 66:1678–1693.
- Erdahl, W. L., C. J. Chapman, R. W. Taylor, and D. R. Pfeiffer. 1995. Effects of pH conditions on  $\text{Ca}^{2+}$  transport catalyzed by ionophores A23187, 4-BrA23187, and ionomycin suggest problems with common applications of these compounds in biological systems. *Biophys. J.* 69:2350–2363.
- Erdahl, W. L., C. J. Chapman, E. Wang, R. W. Taylor, and D. R. Pfeiffer. 1996. Ionophore 4-BrA23187 transports  $\text{Zn}^{2+}$  and  $\text{Mn}^{2+}$  with high selectivity over  $\text{Ca}^{2+}$ . *Biochemistry.* 35:13817–13825.
- Fasolato, C., and T. Pozzan. 1989. Effect of membrane potential on divalent cation transport catalyzed by the “electroneutral” ionophores A23187 and ionomycin. *J. Biol. Chem.* 264:19630–19636.
- Fry, D. W., J. C. White, and D. Goldman. 1978. Rapid separation of low molecular weight solutes from liposomes without dilution. *Anal. Biochem.* 90:809–815.
- Grandjean, J., and P. Laszlo. 1984. Synergistic transport of  $\text{Pr}^{3+}$  across lipid bilayers in the presence of two chemically distinct ionophores. *J. Am. Chem. Soc.* 106:1472–1476.
- Hunt, G. R. A. 1975. Kinetics of ionophore-mediated transport of  $\text{Pr}^{3+}$  ions through phospholipid membranes using  $^1\text{H}$  NMR spectroscopy. *FEBS Lett.* 58:194–196.
- Hunt, G. R. A., and I. C. Jones. 1982. Lanthanide-ion transport across phospholipid vesicular membranes: a comparison of alamethicin 30 and A23187 using  $^1\text{H}$ -NMR spectroscopy. *Sci. Rep.* 2:921–928.
- Hunt, G. R. A., L. R. H. Tipping, and M. R. Belmont. 1978. Rate-determining processes in the transport of  $\text{Pr}^{3+}$  ions by the ionophore A23187 across phospholipid vesicular membranes. A  $^1\text{H}$  NMR theoretical study. *Biophys. Chem.* 8:341–355.
- Jones, E. B. J., D. J. Nelson, and M. M. Turnbull. 1992. Enhancement and quenching of fluorescence of Quin-2 by metal ions. *J. Inorg. Biochem.* 45:85–92.
- Kamo, N., M. Muratsugu, R. Hongoh, and Y. Kobatake. 1979. Membrane potential of mitochondria measured with an electrode sensitive to tetraphenylphosphonium and relationship between proton electrochemical potential and phosphorylation potential in steady state. *J. Membr. Biol.* 49:105–121.
- Kolber, M. A., and D. H. Haynes. 1981. Fluorescence study of the divalent cation transport mechanism of ionophore A23187 in phospholipid membranes. *Biophys. J.* 36:369–391.
- Lehrmann, R., and J. Seelig. 1994. Adsorption of  $\text{Ca}^{2+}$  and  $\text{La}^{3+}$  to bilayer membranes: measurement of the adsorption enthalpy and binding constant with titration calorimetry. *Biochim. Biophys. Acta.* 1189:89–95.
- Lyle, S. J., and M. Rahman. 1963. Complexometric titration of yttrium and the lanthanons. *Talanta.* 10:1177–1182.
- Montal, M. 1970. Experimental membranes and mechanisms of bioenergy transduction. *Annu. Rev. Bioeng.* 5:119–175.
- Perrin, D. D., and I. G. Sayce. 1967. Computer calculation of equilibrium concentrations in mixtures of metal ions and complexing species. *Talanta.* 14:833–842.
- Pfeiffer, D. R., S. M. Hutson, R. F. Kaufman, and H. A. Lardy. 1976. Some effects of ionophore A23187 on energy utilization and the distribution of cations and anions in mitochondria. *Biochemistry.* 15:2690–2697.
- Pfeiffer, D. R., and H. A. Lardy. 1976. Ionophore A23187. The effect of  $\text{H}^+$  concentration on complex formation with divalent and monovalent cations and the demonstration of  $\text{K}^+$  transport in mitochondria mediated by A23187. *Biochemistry.* 15:935–943.
- Pfeiffer, D. R., R. W. Taylor, and H. A. Lardy. 1978. Ionophore A23187: cation binding and transport properties. *Ann. N.Y. Acad. Sci.* 307:402–423.
- Puskin, J. S., and T. E. Gunter. 1975. Electron paramagnetic resonance of copper ion and magnesium ion complexes with A23187. *Biochemistry.* 14:187–191.
- Shastri, B. P., M. B. Sankaram, and K. R. K. Easwaran. 1987. Carboxylic ionophore (lasalocid A and A23187) mediated lanthanide ion transport across phospholipid vesicles. *Biochemistry.* 26:4925–4930.
- Smith, G. D., and W. L. Duax. 1976. Crystal and molecular structure of the calcium complex of A23187. *J. Am. Chem. Soc.* 98:1578–1580.

- Stiles, M. K., M. E. Craig, S. L. N. Gunnell, D. R. Pfeiffer, and R. W. Taylor. 1991. The formation constants of ionomycin with divalent cations in 80% methanol-water. *J. Biol. Chem.* 266:8336–8342.
- Taylor, R. W., R. F. Kaufman, and D. R. Pfeiffer. 1982. Cation complexation and transport by carboxylic acid ionophores. In *Polyether Antibiotics: Naturally Occurring Acid Ionophores*. J. W. Westley, editor. Marcel Dekker, New York. 103–184.
- Thomas, T. P., E. Wang, D. R. Pfeiffer, and R. W. Taylor. 1997. Evidence against formation of A23187 dimers and oligomers in solution: photo-induced degradation of ionophore A23187. *Arch. Biochem. Biophys.* 342:351–361.
- Tissier, C., J. Juillard, D. W. Boyd, and A. M. Albrecht-Gary. 1985. Mode of action of calcimycin (A 23187). II. A study of its interactions with alkali and alkali-earth cations in methanol-water mixtures. *J. Chim. Phys.* 82:899–906.
- Tissier, M., A. Ouahabi, G. Jeminet, and J. Juillard. 1993. Mode of action of calcimycin (A23187). VI. Complexation of transition and heavy metal divalent cations in methanol. *J. Chim. Phys.* 90:595–608.
- Tocanne, J.-F., and J. Teissie. 1990. Ionization of phospholipids and phospholipid-supported interfacial lateral diffusion of protons in membrane model systems. *Biochim. Biophys. Acta.* 1031:111–142.
- Toepfilitz, B. K., A. I. Cohen, P. T. Funke, W. L. Parker, and T. Z. Gougoutas. 1979. Structure of ionomycin—a novel diacidic polyether antibiotic having high affinity for calcium ions. *J. Am. Chem. Soc.* 101:3344–3353.
- Vogel, A. I. 1961. Determination of copper using fast sulphon black F indicator. In *Quantitative Inorganic Analysis*, 3rd ed., Wiley, New York. 415–467.
- Wang, E., and D. R. Pfeiffer. 1996. The transport of lanthanide cations by  $\text{Ca}^{2+}$  ionophores. *Biophys. J.* 70:A366.
- Westley, J. W. 1983. Chemical transformation of polyether antibiotics. In *Polyether Antibiotics, Naturally Occurring Acid Ionophores*. J. W. Westley, editor. Marcel Dekker, New York. 51–86.
- Wrigglesworth, J. M., C. E. Cooper, M. A. Sharpe, and P. Nicholls. 1990. The proteoliposomal steady state: effect of size, capacitance and membrane permeability on cytochrome-oxidase-induced ion gradients. *Biochem. J.* 270:109–118.
- Yuchi, A. A., M. Tanaka, T. Hirai, T. Yasui, H. Wada, and G. Nakagawa. 1993. Complexation equilibria and fluorescent properties of chelating reagents derived from ethylene glycol bis(2-aminoethyl ether)-*N,N,N',N'*-tetraacetic Acid. *Bull. Chem. Soc. Jpn.* 66:3377–3381.